# Improving the Thermodynamic Profiles of Prospective Suzuki-Miyaura Cross-Coupling Catalysts by Altering the Electrophilic Coupling Component

**Dr. Michael Busch,[a,b,c] Dr. Matthew D. Wodrich,[a] and Prof. Dr. Clémence Corminboeuf[a,b]***

[a]Laboratory for Computational Molecular Design, Institute of Chemical Sciences and Engineering, Ecole Polytechnique Fédérale de Lausanne, 1015 Lausanne, Switzerland

[b]National Centre for Computational Design and Discovery of Novel Materials (MARVEL), Ecole Polytechnique Fédérale de Lausanne, 1015 Lausanne, Switzerland

[c]Current Address: Department of Physics, Chalmers University of Technology, Fysikgränd 3, SE-412 96 Göteborg, Sweden

Email: clemence.corminboeuf@epfl.ch

## Abstract

As a heavily used technique for forming new C-C bonds, developing new catalysts and reaction conditions for Suzuki-Miyaura cross-couplings is highly desirable. Here, using molecular volcano plots, the influence of the electrophilic coupling component in catalytic cycle thermodynamics is revealed. Less reactive electrophiles, such as iodine, broaden the volcano plateau, which leads to a larger number of catalysts having appealing thermodynamic profiles. On the other hand, fluorine and other more reactive electrophiles compress the volcano plateau, which shrinks the pool of catalysts having good thermodynamic profiles. As a result, judicious selection of the electrophile employed in a reaction may represent an appealing strategy for further tuning the thermodynamics of cross-coupling reactions.

## Introduction

Suzuki-Miyaura cross-coupling[1] is amongst the most widely used reactions for forming new C-C bonds. Yet, interest persists in developing new catalysts and reaction conditions to accomplish a wide variety of objectives. This is attested to by the increasing number of transition metals[2] and ligands[3] capable of catalyzing these reactions, as well as the development of catalysts capable of operating in an aqueous environment.[4] Density functional theory (DFT) studies have greatly aided experimental investigations in gaining enhanced understanding of catalytic behavior during the cross-coupling process. Specifically, computation have contributed significantly to cross-coupling reactions by assisting in: establishing the viability of different mechanistic pathways,[5] identifying the rate limiting step,[6] better understanding the role played by the solvent,[7] and uncovering the energetic influences accompanying myriad ligand types.[8] Today, computational studies are increasingly used to predict and design new catalysts *in silico*,[9][10] some of which have been experimentally realized.[11]

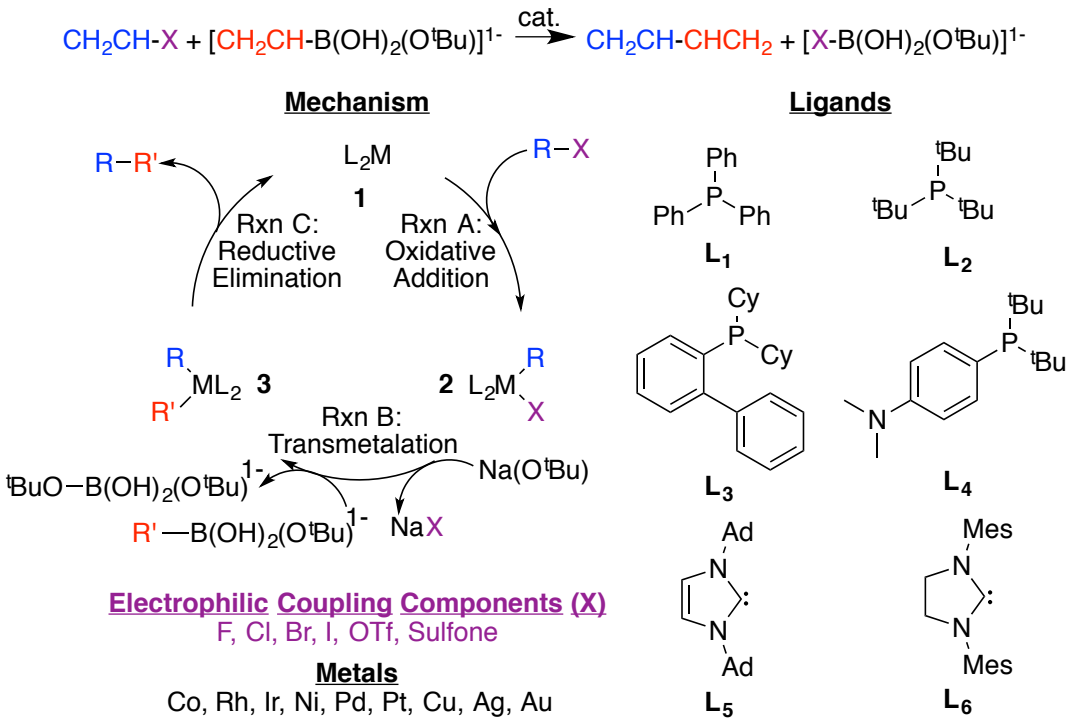


**Scheme 1.** Reaction and key mechanistic steps for Suzuki-Miyaura cross-coupling using various electrophilic coupling components (ECCs), X.

Rather than relying upon combinatorial approaches for computationally designing new catalysts, a systematic method of identifying new species with desired properties would be highly valuable. One tool commonly used in heterogeneous and electrocatalysis[9b, 12] fitting this description is the volcano plot.[13] Built upon linear scaling relationships[14] (akin to Bell-Evans-Polanyi[15] relationships), these plots facilitate the rapid visualization of the properties of prospective catalysts (*e.g.*, appealing thermodynamic profiles, limiting reaction steps, high turnover frequency) based on their location on the volcano. Species in the upper regions, those on or near the volcano plateau or peak, have more attractive characteristics then those in lower areas. In essence, volcano plots pictorially represent Sabatier's principle,[16] which states that an ideal energetic balance exists between a catalyst and a substrate. Overly strong interactions cause product release to be thermodynamically difficult, while overly weak interactions make reactant adsorption difficult. Despite its conceptual simplicity and

widespread use in heterogeneous and electrocatalysis, volcano plots were virtually absent from homogeneous catalysis until 2015,[17] when we showed they could also screen molecular catalysts and assess their thermodynamic profiles.[18] More recently, we demonstrated that utilizing an additional descriptor could also uncover the energetic influence brought about by other reaction components that also influence the catalytic cycle, such as transmetallation agents. This finding facilitated the creation of a generalized thermodynamic picture of C-C cross-coupling reaction variants (*e.g.*, Suzuki, Kumada, Stille, Negishi, Hiyama),[19] which differ in the species used for transmetallation, using three-dimensional volcano plots. The purpose of this article is to demonstrate, using both two- and three-dimensional volcano plots, how alteration of a different component of the reaction mixture, the electrophilic coupling component (ECC) "X" in Scheme 1, can be employed as a general strategy to increase the pool of prospective catalysts with appealing thermodynamic profiles for Suzuki-Miyaura cross-coupling reactions.

## Results and Discussion

To establish the linear free energy scaling relationships (LFESRs) necessary to construct volcano plots, thermodynamic cycles[20] consisting of oxidative addition, transmetalation, and reductive elimination (Scheme 1) were computed using DFT (see Computational Methods section for full details) for 54 catalysts consisting of combinations of Co, Rh, Ir, Ni, Pd, Pt, Cu, Ag, and Au metals along with two bulky phosphine ligands, two Buchwald ligands, and two bulky NHC ligands (Scheme 1). The oxidation states of the catalysts were adjusted to align with 14e-/16e- nature of the coupling reaction by placing charges (-1 for Co, Rh, Ir and +1 for Cu, Ag, Au) on select species. In investigating the influence of the ECC, all species were assumed to be low-spin and to navigate the catalytic cycle as bisligated species. While the exact nature of the active catalyst during the cross-coupling process is a matter of debate, we have found that changes in ligation, oxidation, and spin state do not influence the linear scaling relationships used to construct volcano plots,

provided that the reaction mechanisms remain unchanged.[21] As result, the bis- versus monoligated, low- versus high-spin, and different catalytic oxidation states of catalysts will each appear as separate points on the same volcano plot, but will not impact the shape of the volcano,[21] which is of key importance for this work.

Varying the ECC should change the energies of oxidative addition (Rxn A) and transmetalation (Rxn B), but not reductive elimination (Rxn C), since the ECC leaves the catalytic cycle during transmetalation. Computing each catalytic cycle intermediate (**1**, **2**, **3**) for the 54 catalysts gave rise to LFESRs that establish the differences brought about by using various ECCs. Using simple mathematics (see Supporting Information for derivations), these LFESRs can be converted into volcano plots, which differ based on their ECCS, as seen in Figure 1.

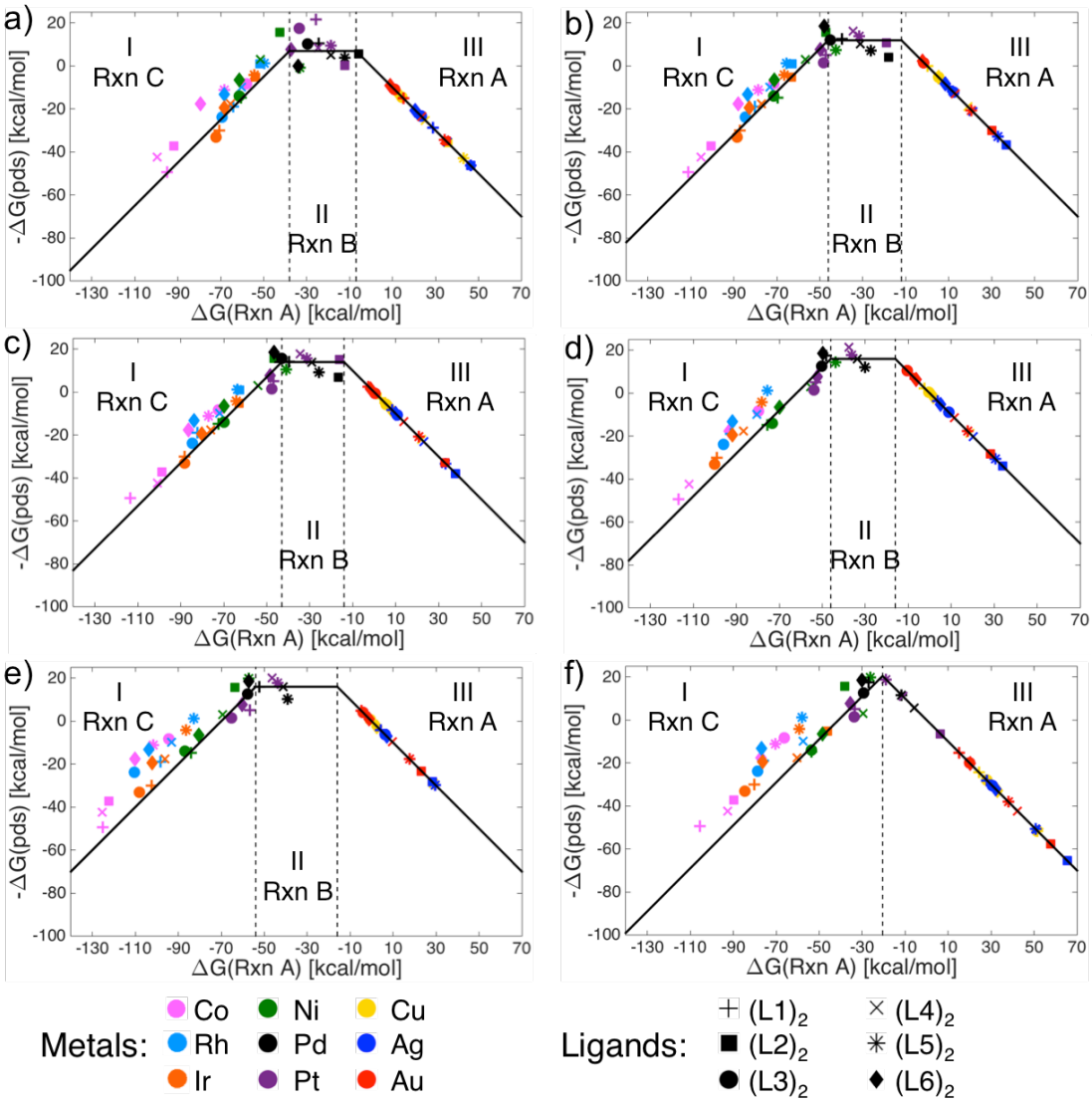


**Figure 1.** Two-dimensional volcano plots for the Suzuki-Miyaura reaction depicted in Scheme with (a) F, (b) Cl, (c) Br, (d) I, (e) OTf, and (f) sulfone electrophilic coupling components. Dashed vertical lines delineate regions where different reactions steps (oxidative addition, transmetalation, reductive elimination) are the thermodynamically most difficult reaction step (potential determining step, pds).

Each volcano plot can be subdivided into three sections related to Sabatier's principle. The "strong-binding" left slope (e.g., "I" in Figure 1) indicates that reductive elimination (Rxn C) is the thermodynamically most difficult reaction step for catalyst lying in this region. In contrast, the "weak-binding" right slope represents situations where the

catalyst/substrate interaction is too weak, thus for catalysts lying in region III, the energy needed to complete oxidative addition (Rxn A) is the thermodynamically most difficult step. Those catalysts lying in region II have "ideally balanced" thermodynamic profiles in which the interaction between the substrate and the catalyst is neither too weak nor too strong, which matches Sabatier's concept of an ideal catalyst. For these species, the energy needed to complete transmetalation (Rxn B) is the most difficult of the catalytic cycle (see Supporting Information for the energies of each reaction step for all tested catalysts).

The simplest way of understanding the volcano plots depicted in Figure 1 is to consider the quantities plotted along their axes. The x-axis displays the magnitude of the catalyst/reactant interaction (*i.e.*, the binding energy), which, in this instance, is equivalent to the energy of oxidative addition (Rxn A). This information makes the shape of the volcano plot readily understandable: for catalysts with endergonic binding energies [$\Delta G(\text{Rxn A}) > 0$] the energy required for oxidative addition is the most costly step in the catalytic cycle. When the energy needed to complete Rxn A becomes more exergonic (*i.e.*, moving leftward along the x-axis) the other catalytic cycle steps (transmetalation followed by reductive elimination) become the most costly. The volcano plot's y-axis represents the energy needed to complete the catalytic cycle's most thermodynamically difficult step [*i.e.*, the potential determining step (pds)]. The specific nature of this step, be it oxidative addition (Rxn A), transmetalation (Rxn B), or reductive elimination (Rxn C), is dictated by the strength of the catalyst/reactant binding energy that is plotted along the x-axis. By convention, the y-axis is given as the negative of the potential determining step [$-\Delta G(\text{pds})$], which means that positive values correspond to exergonic reaction energies. Thus, catalysts that appear high on the volcano plot will, in general, have the most attractive thermodynamic profiles.

Examining the Figure 1 volcano plots in detail reveals both similarities and differences: the overall volcano shapes are quite similar (with the notable exception of sulfone, Figure 1f) but the width and height of the plateau region changes when the ECC is altered. Each of the halogens (Figure 1a-d) display roughly equivalent plateau widths [*i.e.*,

they span a range of binding energies (x-axis) of ~30 kcal/mol] but the height (y-axis) of the plateau increases along the halogen series [-ΔG(pds) = 7 kcal/mol for F, 12 kcal/mol for Cl, 14 kcal/mol for Br, and 16 kcal/mol for I]. This increase in height corresponds to greater exergonicity for the transmetalation step, which is the most difficult in the catalytic cycle for species lying in the plateau region. Indeed, the improved thermodynamic profiles of Br and I align well with the widespread experimental use, while R-F and R-Cl species are generally considered to be poor ECCs that require a judicious choice of catalyst with specific ligands in order to overcome their sluggishness.[22]

Figures 1e and 1f show volcano plots for the triflate and sulfone ECCs. As a pseudohalogen, the triflate volcano is similar to both iodine and bromine and is characterized by a broad plateau with a potential determining step that is 16 kcal/mol exergonic. Analogues to other halogen ECCs, many of the same Pd and Pt catalysts appear in the plateau region corresponding to attractive thermodynamic profiles. This sharply contrasts the shape of the volcano for sulfone, which lacks a plateau region entirely. The characteristic "peak" shape of this plot indicates that only a single catalyst/reactant binding energy (x-axis value) will yield the best possible thermodynamic reaction profile, which corresponds to a location on the summit. Indeed, $Pt(L5)_2$, shown as a purple asterisk in Figure 1f, nearly perfectly matches the binding energy corresponding to the summit, meaning that this catalyst should possess an improved thermodynamic profile relative to other halogen and the triflate ECC (since the peak has a greater y-axis value than the plateaus of the other volcanoes).

While examining any of the Figure 1 two-dimensional volcano plots reveals a substantial amount of information about the behavior of specific catalysts for any cross-coupling process that employees a single ECC, establishing overall thermodynamic trends that identify energetic relationships amongst the different ECCs would be of considerable value for the rational design of new catalytic systems. For example, the 2D volcano plots for iodine and triflate (Figure 1d and 1e) are closely related to one another since they share the same value when transmetalation is the potential determining step (*i.e.*, they have the same

plateau height in region II). The principle difference between the 2D volcanoes for these two ECCs is the broadness of their plateau regions, with triflate spanning a larger range of ΔG(Rnx A) (x-axis) values than for iodine. This increased span directly equates to a larger number of potential catalysts having the best possible thermodynamic profile. Thus, it is clear that broadening the plateau region of the volcano through variation of the ECC could be an easily realizable experimental means toward improving the thermodynamic profiles of prospective catalysts by shifting them from the side of the volcano plot onto the plateau. To fully understand how the size of the plateau regions can be systematically altered, we turn to constructing three-dimensional volcano plots.

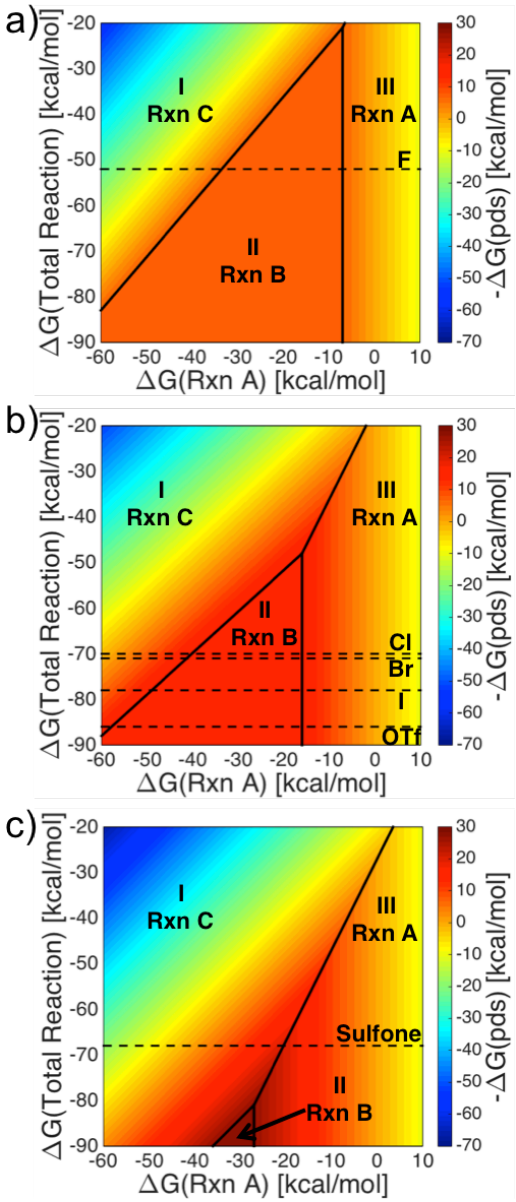


**Figure 2.** Three-dimensional volcano plots using various electrophilic coupling components. The plots differ in the free energy of plateau region (II, Rxn B). Using F as an electrophilic coupling component results in weak thermodynamic drive for the thermodynamically most difficult reaction step (Rxn B, orange color, Figure 2a). The improved energies in the plateau region (II, Rxn B) of Figure 2b indicate that electrophilic coupling components that give more exergonic reaction energies have larger plateau regions, which should results in a larger number of functional catalysts (e.g., Cl versus OTf). Figure 2c shows that sulfone has

tremendous thermodynamic potential (dark red region), but requires a very exergonic total reaction to reach the plateau region (II, Rxn B).

The 3D volcano plots shown in Figure 2 reveal how the catalytic cycle's total reaction energy influences the energies needed to complete each of the individual steps of the cycle for different ECCs. Figure 2a shows a 3D volcano plot for ECCs, such as F, which have weakly exergonic transmetalation steps (*i.e.*, the plateau of the corresponding 2D volcano plots, Figure 1a, lies at -7 kcal//mol). Because the dashed line for the total reaction energy of fluorine [ΔG(Total Reaction) = -52 kcal/mol] crosses region II, the thermodynamics of this ECC can not be further improved (*e.g.*, the overall exergonicity of the most difficult step of the catalytic cycle can not be increased). This is easily visualized by the dashed line crossing the solid orange color, indicative of a region of maximum exergonicity in the 3D volcano. A more exergonic coupling reaction (*i.e.*, a downward shift of the dashed line) would broaden the plateau resulting in catalysts with a greater ranger of catalyst/reactant binding energies (given on the x-axis) falling into the region of maximum exergonicity (region II). In other words, catalysts that fall in area I (where the energy needed to complete the most difficult reaction step of the catalytic cycle is more costly) for a given ΔG(Total Reaction) value can be shifted into a region of increased exergonicity by a downward shift of the dashed line. In contrast, a movement toward less exergonic total reaction energies (corresponding to upward shift of the dashed line) would result in a smaller range of catalyst/reactant interaction falling into the orange region. At the extreme, when ΔG(Total Reaction) becomes greater than -21 kcal/mol, the energy of the most difficult catalytic step (which will always be oxidative addition or reductive elimination) becomes progressively less exergonic.

Figure 2b shows the 3D volcano representing Cl, Br, I, and OTf together in one plot, which is possible because their transmetalation values in the Figure 1 two-dimensional volcano plots are roughly equivalent. Here, it becomes quite evident how increasing ΔG(Total

Reaction) results in broadening of the volcano plateau [since the width of red region II is greater for more exergonic ΔG(Total Reaction)]. A closer examination of the plot reveals that this broadening occurs by a shift of the strong-binding slope toward more exergonic catalyst/reactant binding energies (shown on the x-axis). Thus, the thermodynamic profile of a catalyst that appears in region I when chlorine is used as the ECC can instantly be improved through the use of a more reactive ECC such as iodine or triflate, where the same catalyst/reactant binding energy would place the catalyst on the plateau (region II). The Figure 2b plateau also indicates that the thermodynamics of the most difficult catalytic cycle step is improved relative to fluorine. The plateau (region II) lies at a more exergonic value, which is shown by the darker orange/red color as opposed to lighter orange in Figure 2a.

Finally, the Figure 2c volcano shows the performance of sulfone. Consistent with the two-dimensional volcano (Figure 1f), the free energy of the reaction with sulfone does not cross the small plateau region located at the bottom of Figure 2c. Nonetheless, the peak (located at the intersection of the dashed and solid black lines) has a thermodynamic reaction energy for both oxidative addition (Rxn A) and reductive elimination (Rxn C) that are more exergonic than the potential determining transmetalation steps given in Figures 2a and 2b. More exergonic total reaction energies (*i.e.*, a downward shift on the Figure 2c volcano) would result in a futher increase in thermodynamic drive during the catalytic cycle. Thus, for highly exergonic reactions (e.g., > 65 kcal/mol) using sulfone as an ECC would result in enhanced exergonicity of each of the catalytic cycle steps over more conventionally used ECCs such as bromine, iodine, and triflate. However, owing to the shape of the volcano, only a very select number of catalyst lying within a narrow range of catalyst/reactant binding energies (x-axis) will result in maximum thermodynamic drive.

## Conclusions

In conclusion, we have shown using volcano plots, how judicious choice of the electrophilic coupling component (ECC) in Suzuki-Miyaura cross-coupling reactions can be

used to increase the number of viable catalysts and improve the thermodynamics of their catalytic cycles. The examples provided here further demonstrate how volcano plots, particularly the three-dimensional variant, can be useful both for designing new catalytic reaction conditions and for gaining a better understanding of existing catalytic processes by identifying relationships between cycle energetics and different reaction components that are independent of the catalyst (*e.g.*, the ECC). In the future, we hope to utilize molecular volcano plots to analyze transition-metal catalyzed reactions incorporating multiple catalytic species (tandem catalysis) as well as extend their applicability beyond metal based systems by examining organocatalytic processes.

**Computational Details.** Geometries of all species were optimized at the PBE0[23]-D3[24](BJ)/def2-SVP theoretical level using the SMD[25] solvation model (in THF) in Gaussian09.[26] Reported free energies include unscaled enthalpy correction and entropy correction arising only from vibrational contributions.[27] The scaling of entropy in this manner prevents the overestimation of free energies associated with the dissociation of one species into two molecules (as occurs in reductive elimination) and the underestimation of association reactions (such as oxidative addition). Treating the entropy in this way has previously been employed both by us[19] and others[6a, 28] to study transition-metal-catalyzed reactions.

**Acknowledgments**. The National Centre of Competence in Research (NCCR) "Materials' Revolution: Computational Design and Discovery of Novel Materials (MARVEL)" of the Swiss National Science Foundation (SNSF) and the EPFL are acknowledged for financial support. Mr. Laurent Vannay and Dr. Ganna Gry'nova are acknowledged for technical support and helpful discussions.

## References

[1] a) N. Miyaura, K. Yamada, A. Suzuki, *Tetrahedron Lett.* **1979**, *20*, 3437-3440; b) N. Miyaura, A. Suzuki, *Chem. Rev.* **1995**, *95*, 2457-2483; c) A. Suzuki, *Angew. Chem., Int. Ed.* **2011**, *50*, 6722-6737.

[2] a) R. B. Bedford, S. L. Hazelwood, D. A. Albisson, *Organometallics* **2002**, *21*, 2599-2600; b) J. Zhou, G. C. Fu, *J. Am. Chem. Soc.* **2003**, *125*, 14726-14727; c) J. Zhou, G. C. Fu, *J. Am. Chem. Soc.* **2004**, *126*, 1340-1341; d) B. D. Sherry, A. Fürstner, *Acc. Chem. Res.* **2008**, *41*, 1500-1511; e) P. Garcia, M. Malacria, C. Aubert, V. Gandon, L. Fensterbank, *ChemCatChem* **2010**, *2*, 493-497; f) X. Hu, *Chem. Sci.* **2011**, *2*, 1867-1886; g) R. Jana, T. P. Pathak, M. S. Sigman, *Chem. Rev.* **2011**, *111*, 1417-1492; h) F.-S. Han, *Chem. Soc. Rev.* **2013**, *42*, 5270-5298; i) T. Mesganaw, N. K. Garg, *Org. Process Res. Dev.* **2013**, *17*, 29-39; j) S. Z. Tasker, E. A. Standley, T. F. Jamison, *Nature* **2014**, *509*, 299-309; k) T. Sperger, I. A. Sanhueza, I. Kalvet, F. Schoenebeck, *Chem. Rev.* **2015**, *115*, 9532-9586; l) I. Bauer, H.-J. Knölker, *Chem. Rev.* **2015**, *115*, 3170-3387; m) O. M. Kuzmina, A. K. Steib, A. Moyeux, G. Cahiez, P. Knochel, *Synthesis* **2015**, *47*, 1696-1705; n) Ni- and Fe- Based Cross-Coupling Reactions, Vol. 374 (Ed.: A. Correa), Springer International Publishing, 2016; o) C. Cassani, G. Bergonzini, C.-J. Wallentin, *ACS Catal.* **2016**, *6*, 1640-1648.

[3] a) M. Miura, *Angew. Chem., Int. Ed.* **2004**, *43*, 2201-2203; b) T. E. Barder, S. D. Walker, J. R. Martinelli, S. L. Buchwald, *J. Am. Chem. Soc.* **2005**, *127*, 4685-4696; c) A. Fihri, P. Meunier, J.-C. Hierso, *Coord. Chem. Rev.* **2007**, *251*, 2017-2055; d) E. A. B. Kantchev, C. J. O'Brien, M. G. Organ, *Angew. Chem., Int. Ed.* **2007**, *46*, 2768-2813; e) G. C. Fu, *Acc. Chem. Res.* **2008**, *41*, 1555-1564; f) R. Martin, S. L. Buchwald, *Acc. Chem. Res.* **2008**, *41*, 1561-1473; g) D. S. Surry, S. L. Buchwald, *Angew. Chem., Int. Ed.* **2008**, *47*, 6338-6361; h) M.-N. Birkholz, Z. Freixa, P. W. N. M. van Leeuwen, *Chem. Soc. Rev.* **2009**, *38*, 1099-1118; i) C. Valente, S. Çalimsiz, K. H. Hoi, D. Mallik, M. Sayah, M. G. Organ, *Angew. Chem., Int. Ed.* **2012**, *51*, 3314-3332.

[4] a) Q. Liang, P. Xing, Z. Huang, J. Dong, K. B. Sharpless, X. Li, B. Jiang, *Org. Lett.* **2015**, *17*, 1942-1945; b) A. Chatterjee, T. R. Ward, *Catal. Lett.* **2016**, *146*, 820-840; c) Z. Li, C. Gelbaum, J. S. Fisk, B. Holden, A. Jaganathan, G. T. Whiteker, P. Pollet, C. L. Liotta, *J. Org. Chem.* **2016**, *81*, 8520-8529; d) Z. Li, C. Gelbaum, W. L. Heaner IV, J. S. Fisk, A. Jaganathan, B. Holden, P. Pollet, C. L. Liotta, *Org. Process Res. Dev.* **2016**, *20*, 1489-1499.

[5] a) L. J. Gooßen, D. Koley, H. L. Hermann, W. Thiel, *Chem. Commun.* **2004**, 2141-2143; b) L. J. Goossen, D. Koley, H. L. Hermann, W. Thiel, *Organometallics* **2005**, *24*, 2398-2410; c) A. A. C. Braga, N. H. Morgon, G. Ujaque, F. Maseras, *J. Am. Chem. Soc.* **2005**, *127*, 9298-9307; d) A. A. C. Braga, N. H. Morgon, G. Ujaque, A. Lledós, F. Maseras, *J. Organomet. Chem.* **2006**, *691*, 4459-4466; e) K. C. Lam, T. B. Marder, Z. Lin, *Organometallics* **2007**, *26*, 758-760; f) C. Sicre, A. A. C. Braga, F. Maseras, M. M. Cid, *Tetrahedron* **2008**, *64*, 7437-7443; g) M. Pérez-Rodríguez, A. A. C. Braga, M. Garcia-Melchor, M. H. Pérez-Temprano, J. A. Casares, G. Ujaque, A. R. de Lera, R. Álvarez, F. Maseras, P. Espinet, *J. Am. Chem. Soc.* **2009**, *131*, 3650-3657; h) C. L. McMullin, J. Jover, J. N. Harvey, N. Fey, *Dalton Trans.* **2010**, *39*, 10833-10836; i) C.-M. Weng, F.-E. Hong, *Dalton Trans.* **2011**, *40*, 6458-6468; j) M. A. Ortuño, A. Lledós, F. Maseras, G. Ujaque, *ChemCatChem* **2014**, *6*, 3132-3138.

[6] a) A. A. C. Braga, G. Ujaque, F. Maseras, *Organometallics* **2006**, *25*, 3647-3658; b) M. A. Düfert, K. L. Billingsley, S. L. Buchwald, *J. Am. Chem. Soc.* **2013**, *135*, 12877-12885.

[7] a) H. M. Senn, T. Ziegler, *Organometallics* **2004**, *23*, 2980-2988; b) F. Proutiere, F. Schoenebeck, *Angew. Chem., Int. Ed.* **2011**, *50*, 8192-8195; c) E. Lyngvi, F. Schoenebeck, *Tetrahedron* **2013**, *69*, 5715-5718.

[8] a) Y.-L. Huang, C.-M. Weng, F.-E. Hong, *Chem. - Eur. J.* **2008**, *14*, 4426-4434; b) J. Jover, N. Fey, M. Purdie, G. C. Lloyd-Jones, J. N. Harvey, *J. Mol. Catal. A* **2010**, *324*, 39-47; c) C. L. McMullin, N. Fey, J. N. Harvey, *Dalton Trans.* **2014**, *43*, 13545-13556.

[9] a) K. N. Houk, P. H.-Y. Cheong, *Nature* **2008**, *455*, 309-313; b) J. K. Nørskov, T. Bligaard, J. Rossmeisl, C. H. Christensen, *Nat. Chem.* **2009**, *1*, 37-46; c) K. A. Murray, M. D. Wodrich, X. Hu, C. Corminboeuf, *Chem. - Eur. J.* **2015**, *21*, 3987-3996.

[10] Also see a special issue entitled: "Computational Catalysis for Organic Synthesis" in *Accounts of Chemical Research* (*Acc. Chem. Res.* **2016**, *49*).

[11] a) J. Sehested, K. E. Larsen, A. L. Kustov, A. M. Frey, T. Johannessen, T. Bligaard, M. P. Andersson, J. K. Nørskov, C. H. Christensen, *Top. Catal.* **2007** *45*, 9-13; b) T. Xu, C.-J. M. Yin, M. D. Wodrich, S. Mazza, K. M. Schultz, R. Scopelliti, X. Hu, *J. Am. Chem. Soc.* **2016**, *138*, 3270-3273.

[12] a) H. Dau, C. Limberg, T. Reier, M. Risch, S. Roggan, P. Strasser, *ChemCatChem* **2010**, *2*, 724-761; b) J. Greeley, N. M. Markovic, *Energy Environ. Sci.* **2012**, *5*, 9246-9256.

[13] a) H. Gerischer, *Bull. Soc. Chim. Belg.* **1958**, *67*, 506-527; b) R. Parsons, *Trans. Faraday Soc.* **1958**, *54*, 1053-1063.

[14] I. C. Man, H.-Y. Su, F. Calle-Vallejo, H. A. Hansen, J. I. Martínez, N. G. Inoglu, J. Kitchin, T. F. Jaramillo, J. K. Nørskov, J. Rossmeisl, *ChemCatChem* **2011**, *3*, 1159-1165.

[15] a) R. P. Bell, *Proc. R. Soc. London, Ser. A* **1936**, *154*, 414-429; b) D. J. Evans, M. Polanyi, *Trans. Faraday Soc.* **1938**, *34*, 11-24.

[16] a) P. Sabatier, *Ber. Deutsch. Chem. Gesellshaft* **1911**, *44*, 1984-2001; b) P. Sabatier, *La Catalyse en Chimie Organique*, Librarie Polytechnique, Paris, **1913**.

[17] Volcano plots for homogeneous catalysis were previously proposed in a hypothetical sense and have recently been discussed within the context of the Energetic Span Model (S. Kozuch, S. Shaik, Acc. Chem. Res. 2011, 44, 101.). See: G. F. Swiegers, Mechanical Catalysis: Methods of Enzymatic, Homogeneous, and Heterogeneous Catalysis, John Wiley & Sons, Hoboken, NJ, 2008 and S. Kozuch in Understanding Organometallic Reaction Mechanisms and Catalysis: Computational and Experimental Tools (Ed. V. P. Ananikov) Wiley-VCH, Weinheim, 2015.

[18] M. Busch, M. D. Wodrich, C. Corminboeuf, *Chem. Sci.* **2015**, *6*, 6754-6761.

[19] M. Busch, M. D. Wodrich, C. Corminboeuf, *ACS Catal.* **2017**, *7*, 5643-5653.

[20] The use of a thermodynamic only picture to assess the behavior of catalysts has both benefits and drawbacks. We recommend the interested reader consult the "Free energy plots" section of reference 18 for a more comprehensive discussion of these points. Volcano plots can also be created to directly predict the kinetic properties of catalysts, albeit at greater computational cost. For more information on kinetic volcano plots for homogeneous catalysis see: M. D. Wodrich, M. Busch, C. Corminboeuf, *Chem. Sci.*, **2016**, *7*, 5723-5735.

[21] M. D. Wodrich, B. Sawatlon, M. Busch, C. Corminboeuf, *ChemCatChem* **2018**, DOI:10.1002/cctc.201701709.

[22] a) N. Yoshikai, H. Matsuda, E. Nakamura, *J. Am. Chem. Soc.* **2009**, *131*, 9590-9599; b) A. F. Littke, G. C. Fu, *Angew. Chem., Int. Ed.* **2002**, *41*, 4176-4211.

[23] a) J. P. Perdew, K. Burke, M. Ernzerhof, *Phys. Rev. Lett.* **1996**, *77*, 3865-3868; b) C. Adamo, V. Barone, *J. Chem. Phys.* **1999**, *110*, 6158-6170.

[24] a) S. Grimme, J. Antony, S. Ehrlich, H. Krieg, *J. Chem. Phys.* **2010**, *132*, 154104; b) S. Grimme, S. Ehrlich, L. Goerigk, *J. Comput. Chem.* **2011**, *32*, 1456-1465.

[25] A. V. Marenich, C. J. Cramer, D. G. Truhlar, *J. Phys. Chem. B* **2009**, *113*, 6378-6396.

[26] M. J. Frisch, G. W. Trucks, H. B. Schlegel, G. E. Scuseria, M. A. Robb, J. R. Cheeseman, G. Scalmani, V. Barone, B. Mennucci, G. A. Petersson, et al., Gaussian, Inc., Wallingford, CT, **2009**.

[27] This quantity can be obtained directly from a Gaussian output file by taking only the "Vibrational" contribution to the entropy (S), rather than the "Total" contribution.

[28] a) H. Tamura, H. Yamazaki, H. Sato, S. Sakaki, *J. Am. Chem. Soc.* **2003**, *125*, 16114-16126; b) S. Sakaki, T. Takayama, M. Sumimoto, M. Sugimoto, *J. Am. Chem. Soc.* **2004**, *126*, 3332-3348; c) M. Sumimoto, N. Iwane, T. Takhama, S. Sakaki, *J. Am. Chem. Soc.* **2004**, *126*, 10457-10471.

TOC Graphic:

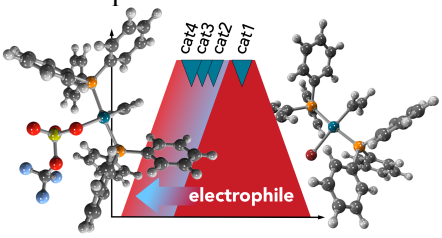


TOC Text: **Broad is beautiful!** Varying the electrophile in Suzuki-Miyaura cross-coupling reactions expands to the top of the volcano plateau where catalysts with the most appealing thermodynamic profiles lie. Thus, adjusting the electrophile might represent a useful strategy to improve the performance of sluggish catalysts.

Keywords: homogeneous catalysis, density functional calculations, transition metals, linear scaling relationships, cross-coupling